

The Mars Observer Differential One-Way Range Demonstration

P. M. Kroger and J. S. Border
Tracking Systems and Applications Section

S. Nandi
Earth Observations Analysis Systems Section

Current methods of angular spacecraft positioning using station differenced range data require an additional observation of an extragalactic radio source (quasar) to estimate the timing offset between the reference clocks at the two Deep Space Stations. The quasar observation is also used to reduce the effects of instrumental and media delays on the radio metric observable by forming a difference with the spacecraft observation (delta differential one-way range, ΔDOR). An experiment has been completed using data from the Global Positioning System satellites to estimate the station clock offset, eliminating the need for the quasar observation. The requirements for direct measurement of the instrumental delays that must be made in the absence of a quasar observation are assessed. Finally, the results of the "quasar-free" differential one-way range, or DOR, measurements of the Mars Observer spacecraft are compared with those of simultaneous conventional ΔDOR measurements.

I. Introduction

The state of an interplanetary spacecraft can be inferred from Doppler and range data recorded at a single Deep Space Station (DSS) of the DSN. The information content of single-station observations is mainly along the direction of the spacecraft line of sight, although the angular position can be inferred from the diurnal signature in the Doppler data [1]. Direct estimation of the angular position of a spacecraft may be accomplished with the use of station-differenced range data. One such technique has been adopted for operational use by the DSN [2,3]. Referred to as delta differential one-way range (ΔDOR), this method uses the recorded phase (range) of side tones or subcarrier harmonics of the spacecraft's telemetry signal to estimate the difference in the time of arrival, or

delay, of these signals at a pair of Deep Space Stations (Fig. 1). As indicated in Fig. 1, an additional observation of an extragalactic radio source or quasar is required to form the final ΔDOR observable: a difference between the spacecraft and quasar delays. This "differential" delay is related to the positions of the spacecraft and quasar on the plane of the sky and the relative positions of the Deep Space Stations by

$$\Delta\tau_{\Delta DOR} = \tau_{SC} - \tau_{egrs} = \frac{\mathbf{B} \cdot (\hat{\mathbf{S}}_{SC} - \hat{\mathbf{S}}_{egrs})}{c} \quad (1)$$

where τ_{SC} is spacecraft delay, τ_{egrs} is quasar delay, c is the speed of light, $\hat{\mathbf{S}}_{egrs}$ and $\hat{\mathbf{S}}_{SC}$ are unit vectors in the direc-

tions of the quasar and spacecraft, respectively, and \mathbf{B} is the baseline vector between the two Deep Space Stations.

The additional quasar observation is necessary for two reasons. Correlation of the broadband noise signal of the quasar recorded at the two Deep Space Stations allows the timing or "clock" offset between them to be estimated. Taking the difference between the spacecraft and quasar delays produces an observable, $\Delta\tau_{\Delta DOR}$, that is nearly free of media and instrumental delay effects common to both the spacecraft and quasar signals. It is this differencing which in fact allows this technique to measure spacecraft positions with an accuracy approaching 5 nrad in the quasar reference system.

The requirement of an additional quasar observation has several drawbacks that affect the utility of this technique in operational spacecraft tracking. First, the tracking antenna must point away from the spacecraft during the time of the quasar observation. The resulting loss of lock on the spacecraft carrier interrupts the transmission of telemetry data to the ground station during this period. Furthermore, the DSN must have a catalog of quasar positions to ensure that a sufficient number of natural radio sources of known source strength, whose positions are accurately known and near to the spacecraft trajectory, are available throughout the duration of each mission. Because a natural radio source's brightness changes with time, a continuing series of radio interferometric measurements of the source strengths is required to "maintain" this catalog. Processing the quasar signal to estimate the delay and clock offset also requires specialized hardware in the form of the Block 1 very long baseline interferometry (VLBI) correlator [4].

For these reasons, it would be valuable in terms of reduced cost and increased operational utility to be able to measure the angular position of a spacecraft without the need for an accompanying radio source observation, and this is the primary motivation for the work described here. What is required is an alternate means to accomplish what the quasar observation now does: measure the clock offset between the Deep Space Stations and remove the effects of instrumental and media delays from the spacecraft delay observable. A clock offset with an accuracy of 1 nsec, neglecting all other error sources, would yield an angular accuracy of about 50 nrad, sufficient for many future missions, especially during their cruise phase.

In the work described in this article, clock offsets determined by analysis of data from the Global Positioning System (GPS) of satellites recorded by receivers located at the Deep Space Stations have been used in place of the

clock offsets normally obtained from quasar observations in conventional ΔDOR measurements. In addition, daily measurements of instrumental timing offsets at the Goldstone, California, and Canberra, Australia, Deep Space Communications Complexes (DSCCs) and the analyses of locally generated calibration tones were made to assess the stability of these delays on a day-to-day basis and determine whether it is feasible to use such measurements to calibrate instrumental effects without a quasar-differenced ΔDOR observable.

II. The Mars Observer Differential One-Way Range Demonstration

During the cruise phase of the Mars Observer (MO) mission, conventional ΔDOR measurements were made on a weekly basis as specified in the overall mission navigation plan.¹ Coincident with these measurements, an attempt was made to perform "quasar-free" differential one-way range (DOR) measurements by recording the phase of several spacecraft tones and combining these with estimates of the station time offsets obtained from analysis of data from the GPS satellites. An important part of this demonstration was the use of the Experimental Tone Tracker (ETT). This remotely controlled device consists of a modified TurboRogue GPS receiver with the capability to acquire and track spacecraft signals at either 2.3 GHz (S-band) or 8.4 GHz (X-band) in two separate baseband channels. ETTs were installed at both the Goldstone and Canberra Deep Space Stations to support this demonstration.

A. Experimental Description

Figure 2 is a schematic diagram of the experimental setup used for recording the Mars Observer spacecraft signals and identifies the instrumental delay measurements that were also made as part of the demonstration. Commands downloaded to the ETTs from JPL contain information on the predicted frequencies of the spacecraft tones that are used by the digital phase-locked loop to acquire the spacecraft signals. Figure 3 is a schematic diagram of the ETT and how it is connected to the radio frequency system of the DSN radio antenna. The radio metric data, consisting of the amplitude, phase, and frequency of the spacecraft signals, are stored in the memory of the ETT and subsequently transferred to a personal computer at JPL through a high-speed modem. The direct transfer of

¹M. J. Rokey, ed., *Mars Observer Mission Plan*, Mars Observer Project Document 642-311 (internal document), Jet Propulsion Laboratory, Pasadena, California, July 1992.

the data and the ability to remotely control the receiver from JPL permit a very efficient method of acquiring and processing radio metric data, requiring a minimum number of personnel at JPL and the Deep Space Stations.

B. DOR Observable

The spacecraft delay, or DOR, observable is formed from the measured phases of spacecraft tones in the same manner as in a conventional Δ DOR measurement. A group delay is computed by taking the difference of the station-differenced phases of two spacecraft tones at their received frequencies and dividing this quantity by the transmitted frequency difference of the tones [3]:

$$\tau_{DOR}(\nu_i, \nu_j; t) = \frac{(\phi_1(\nu_i; t) - \phi_2(\nu_i; t)) - (\phi_1(\nu_j; t) - \phi_2(\nu_j; t))}{\nu_c(m_i - m_j)} \quad (2)$$

where $\phi_1(\nu_i; t)$, $\phi_1(\nu_j; t)$, $\phi_2(\nu_i; t)$, and $\phi_2(\nu_j; t)$ are the phases of tones i and j at time t at stations 1 and 2, ν_c is the transmitted carrier frequency, m_i and m_j are the multipliers that relate the carrier frequency to the side-tone frequencies, and τ_{DOR} is the spacecraft or DOR delay for tones i and j at time t .

A number of delay observables, with different delay ambiguities, can be formed from combinations of the four tones recorded for the MO measurements. The most precise delay is formed from the tone pair with the widest separation (23.1 MHz), but the delays from the more closely spaced tones are needed to resolve the delay ambiguities.

Knowledge of the instrumental delays introduced by the receiving system at the Deep Space Stations is critical in computing an accurate DOR delay observable. The schematic diagram in Fig. 4 shows how a number of instrumental delay terms and timing offsets contribute to the total DOR delay of Eq. (2) that can be expressed as:

$$\begin{aligned} \tau_{DOR}(\nu_i, \nu_j; t) &= \tau_{DOR}^0(\nu_i, \nu_j; t) \\ &+ \Delta\tau_{FE}(\nu_i, \nu_j; t) + \Delta\tau_I(\nu_i, \nu_j; t) \\ &+ \Delta\tau_C(t) - \Delta\tau_E(t) + \Delta\tau_{\text{misc}}(t) + \eta \end{aligned} \quad (3)$$

where τ_{DOR} is the observed spacecraft delay and τ_{DOR}^0 is the model delay computed from a priori knowledge of the geometry of the spacecraft and the locations of Deep Space Stations. The other terms in Eq. (3) are

- (1) $\Delta\tau_{FE}$ is the instrumental delay above the phase-calibration tone injection point. This also includes the delay between the antenna reference point used to compute the baseline vector, \mathbf{B} , and the phase-calibration injection point.
- (2) $\Delta\tau_I$ is the instrumental delay from the phase-calibration tone injection point to the ETT data sampler.
- (3) $\Delta\tau_C$ is the timing or clock offset between the master clocks of the Deep Space Stations.
- (4) $\Delta\tau_E$ is the timing offset between the ETT data sampler and the station's master clock.
- (5) $\Delta\tau_{\text{misc}}$ represents a number of miscellaneous delays including electronic delays within the Rogue GPS receiver and the Experimental Tone Tracker.
- (6) η is a random quantity representing all measurement errors.

As indicated in Eq (3), these delays may be both time and frequency dependent. It was far beyond the scope of this first DOR demonstration to measure all the terms listed above. The DOR delay of Eq. (2) measured in this demonstration is therefore "biased" by the uncalibrated delays and timing offsets. It is crucial to the interpretation of the results of this demonstration to understand what terms in Eq. (3) were not measured. These included items (1) and (5) from the above list. The total magnitude of these terms may be on the order of 1 μ sec, but their variation is expected to be less than 1 nsec. The DOR bias could easily be estimated by comparing the DOR and Δ DOR measurements, as was done in this demonstration (see Section VI). The bias should be independent of the spacecraft and, as shown in Section VI, remain constant over long periods of time.

The measurement of the instrumental delay, $\Delta\tau_I$, provided by the phase-calibration tones was itself biased by the uncalibrated uplink delay, τ_u , and the timing offset between the station master clock, τ_C , and the clock reference of the calibration tone generator, τ_C^p , as shown in Fig. 4. Hence, the delay measured by the phase-calibration tones is actually

$$\tau_\phi = \tau_I + \tau_u - \tau_E - \tau_C^\phi \quad (4)$$

where τ_ϕ is the delay computed from analysis of the phase-calibration tones, τ_u is the uplink delay, τ_E is the timing offset between the ETT and the station master clock, and τ_C^ϕ is the offset between this clock and the reference clock of the tone generator. A complete discussion of the instrumental delays computed from the phase-calibration tones is provided in Section V.B.

It should be noted that the Δ DOR observable is not contaminated by these instrumental delays and timing offsets because they are common to both the spacecraft and quasar signals and are removed when these delays are differenced, as in Eq. (1). A comparison of the Δ DOR delays with the DOR delays will therefore provide an estimate of the magnitude and variability of the uncalibrated delay terms of Eq. (3).

III. Mars Observer DOR Measurements

Table 1 is a summary of the Mars Observer DOR measurements that were completed during the period March 21, 1993, to August 16, 1993. Each measurement consisted of two spacecraft scans separated by the quasar observation required by the concurrent conventional Δ DOR observations.

During the spacecraft observations, the ETT receiver was programmed to record the amplitude and phase of four spacecraft tones, including the 8.4-GHz carrier and three side or "DOR" tones. Figure 5 shows the baseband frequencies (ν_{BB}) of these tones within the 40-MHz intermediate frequency (ν_{IF}) bandpass of the DSN intermediate frequency (IF) system.

IV. GPS Clock Offsets

The $\Delta\tau_C$ term in Eq. (3), representing the timing offset between the Deep Space Stations, is expected to be one of the largest and most time variable of the delays in this equation. Though the other delay terms in Eq. (3) may be of comparable magnitude, they are expected to remain relatively constant over long periods of time and need be measured only infrequently. The time or "clock" offset, $\Delta\tau_C$, however, must be directly measured during the actual DOR measurement since its time variability can be large and it is not predictable at the nanosecond level. Fortunately, the arrival of the GPS system of satellites provides a way to directly measure the time offset between widely separated sites with subnanosecond accuracy [5].

For this demonstration, analysis of data from a global network of GPS receivers [6], which included the DSN Rogue receivers, was used to estimate the timing offset between the Goldstone and Canberra reference clocks at the time of each MO DOR observation. To relate the GPS estimated clock solutions to the station master clock, the time delay between the GPS receiver and the Deep Space Station's reference clock (τ_R in Fig. 4) was also measured.

Figure 6 shows estimates of the clock offset between the Canberra and Goldstone reference clocks obtained by combining the Rogue GPS clock solutions and the measured time delay, τ_R , between the Rogue receivers and the stations' clock reference point (Fig. 2). The Rogue receiver clock offsets have been corrected for the timing offset between the station master clock (Fig. 4) and the Rogue receiver. The abrupt changes in the value of the Rogue GPS clock offsets are most likely due to errors in the measurement of this timing offset and do not reflect changes in the Rogue GPS clock solution. The Rogue clock offsets are determined from the analysis of GPS data from a worldwide network of over 40 receivers. Also shown on this plot are the clock offsets determined by the DSN's own GPS measurement system, which uses the more conventional, but less accurate, "common view" technique.² The greater accuracy of the clock offsets estimated from the Rogue receiver data is evident from the much lower scatter in these clock offsets compared to those determined by the frequency and timing subsystem (FTS). An examination of differences between the FTS and Rogue clock offsets shows a scatter of approximately 15 nsec. That this scatter is dominated by the FTS clock estimates was confirmed by examination of the residuals to a polynomial fit of a 3-day span of Rogue clock offsets. The scatter in the Rogue residuals was approximately 0.2 nsec, consistent with the formal errors reported for these clock solutions.

The large jumps in the Rogue receiver clock offsets that are apparent in Fig. 6 are artifacts introduced by the measurement of the τ_R delay shown in Fig. 4 and do not represent true changes in the clock offset. No abrupt changes are seen in the FTS clock offsets, which use a single value for the equivalent τ_R delay term.

V. Instrumental Delay Calibrations

A. Timing Offset Measurements

Although it was not possible to measure all the delays and timing offsets shown in Fig. 4 and Eq. (3), a number of

²G. A. Santana, personal communication, TDA Mission Support and DSN Operations Section, Jet Propulsion Laboratory, Pasadena, California, December 13, 1993.

timing offsets were measured on a daily basis throughout the 8-month span of the Mars Observer cruise phase. The primary purpose of these daily measurements was to assess the long- and short-term variability of these and similar timing offsets. Figure 7 shows how the measurements were made using a time-interval counter with an accuracy of 100 psec. It was expected that the timing offsets would remain constant at a level of 1 nsec or less over the course of these measurements.

Figure 8, for example, shows the results of the daily measurement of the τ_E delay of Eq. (3) during the period from February 15, 1993, through August 16, 1993, for both the Canberra and Goldstone Deep Space Stations. The measurements were performed with the experiment setup shown in Fig. 7. The day-to-day variability in this delay, as measured at the Canberra Deep Space Station, is extremely small, probably less than 1 nsec. There does appear to be a slight long-term increase in this delay that is not presently understood. In the case of the Goldstone station, there initially appeared to be large variations in this delay in comparison to the Canberra results. After day of year (DOY) 162, however, this variability greatly decreased for reasons yet unknown. The greater variability in the Goldstone delays is probably a result of the measurement procedure and is not a true measure of the variability of this delay. The timing offset measurements at Canberra were completely automated. At Goldstone, these measurements were made manually each day by different station personnel. There are certainly no a priori reasons to expect the large variations in these timing measurements that were reported at the Goldstone Deep Space Station. It is now believed that the measurement methodology was not subject to strict configuration control.³ This was caused by noise in the 1-pulse/sec output of the Rogue receiver at Goldstone that necessitated adjustments to the trigger level of the time interval counter, which may have contributed to the large variation seen in the timing offsets measured at Goldstone in the early part of this demonstration.

B. Instrumental Delay Measurements

The delay introduced into the spacecraft signal as it traverses the electronic components of the receiving system before being sampled and recorded in the ETT memory is represented by the term $\Delta\tau_I$ in Eq. (3). This delay cannot be directly measured in the manner of the timing offsets discussed above. Instead, a comb of calibration tones sep-

arated by 0.1 MHz and spanning the entire bandwidth of the radio-frequency system is injected near the antenna front end (Fig. 3).

These "phase-calibration" tones experience the same instrumental delays as the spacecraft tones, and their phase and amplitude can be recorded by the ETT receiver in the same manner. The use of these tones to calibrate instrumental delays has been a part of the DSN VLBI system since its inception [7]. Because they are derived from the station's hydrogen maser frequency standard, the tones should exhibit stable amplitude and phase over extended periods of time. As discussed in Section II.B, the delay that is measured through analysis of the phase-calibration tone data is not identically the τ_I term of Eq. (3), but is the biased delay of Eq. (4).

In the MO DOR demonstration, the only information on the instrumental delay term τ_I comes from measurement of the phase-calibration tones. During the actual Mars Observer DOR observations, these tones were turned off to prevent the stations' telemetry receivers from inadvertently locking to one of these tones instead of the spacecraft carrier. Measurements of the phase-calibration tones were restricted to the "precalibration" period, which might precede the spacecraft observations by several hours, under the assumption that the instrumental delays will not undergo significant changes in the period before and during the 40-min Δ DOR measurement that follows. This assumption was tested and confirmed by independent measurements of the phase and amplitude of these tones over periods of several hours, where it was shown that the relative phases of the tones remained constant over periods of several hours.⁴

In spite of this, significant problems were faced in the use of the phase-calibration tones to measure the instrumental delay term of Eq. (3) apart from the bias discussed earlier. Initially, it was believed that the instrumental phase could be calibrated by measuring the phase of calibration tones whose baseband frequencies were close to the spacecraft tone frequencies. This method was discussed in an earlier status report on the MO DOR demonstration.⁵ The basic idea, as described there, is to compute a mean spacecraft frequency for each DOR tone and interpolate the instrumental phase correction from the measured phases of calibration tones that are close in fre-

³ M. Manning, personal communication, TDA Mission Support and DSN Operations Section, Jet Propulsion Laboratory, Pasadena, California, January 21, 1994.

⁴ S. Nandi, P. M. Kroger, and J. S. Border, "Mars Observer Differential One-way Ranging Experimental Investigation: Status as of 6-4-93," JPL Interoffice Memorandum 335.1-93-20, Jet Propulsion Laboratory, Pasadena, California, June 28, 1993.

⁵ Ibid.

quency to the spacecraft tone frequency. In this case, the instrumental delay correction is given by

$$\Delta\tau_\phi(\nu_i, \nu_j) = \frac{[\phi_{cal,1}(\nu_i) - \phi_{cal,1}(\nu_j)] - [\phi_{cal,2}(\nu_i) - \phi_{cal,2}(\nu_j)]}{\nu_c(m_i - m_j)} \quad (5)$$

where $\Delta\tau_\phi$ is the estimated instrumental delay correction, $\phi_{cal,1}$ and $\phi_{cal,2}$ are phases obtained by interpolating the measured phase-calibration tone phases at stations 1 and 2 (after the cycle ambiguities have been resolved) to the mean spacecraft tone frequencies ν_i and ν_j , ν_c is the best estimate of the spacecraft carrier frequency, and m_i and m_j are the multipliers that relate the carrier frequency to the DOR tone frequencies for tones i and j . It was found that delays computed in this manner for a number of tone pairs showed variations that were much larger than expected.⁶ That this could be attributed to errors in the ETT tone phase measurement was confirmed to some degree by comparison of calibration tone phases measured by the ETT with those measured simultaneously by the DSN's narrow-band VLBI system during regular VLBI clock-synchronization measurements. This comparison indicated the presence of errors in the ETT's calibration tone-phase measurement on the order of several hundredths of a cycle (Figs. 9 and 10). Phase errors of this magnitude can translate into instrumental delay errors that exceed the 1-nsec goal of this demonstration. Based upon Eq. (5), the relation between the phase error and the delay error is given by

$$\sigma_\tau(\nu_i, \nu_j) = \frac{\sqrt{2}\sqrt{2}\sigma_\phi}{\nu_i - \nu_j} \quad (6)$$

The maximum frequency spacing for the MO DOR tones is approximately 23.1 MHz. This requires a phase accuracy of at least 0.01 cycle to achieve a 1-nsec delay error. The comparison of the ETT phase measurement with the DSN's narrow-channel bandwidth (NCB) VLBI measurements of the same tone phases, however, appears to indicate that ETT tone phases may have errors as large as 0.05 cycle. The reasons for errors of this magnitude are not completely understood, but may be related to the 1-bit data quantization and the 3-level tone stopping function that is used in the ETT, compared to the 128-level stopping function used in the NCB VLBI system. The fact that each ETT channel contains 160 phase-calibration

tones (and all of their intermodulation products) while each NCB channel contains only 2 tones may also contribute to errors in the ETT tone-phase measurement. In any case, the above method of instrumental delay calibration did not provide 1-nsec delay accuracy.

Until the problems with the ETT phase measurements are resolved, the use of the phase-calibration tone phases recorded by the ETT to compensate for instrumental group delays remains problematic. For the purposes of this demonstration, all the calibration tone phases recorded in each ETT channel were simply fit to a line whose slope was taken as an estimate of the group delay for that channel. This was done for the phase-calibration tones recorded during the precalibration period of all DOR measurements listed in Table 1. Figure 11 is a typical plot produced from calibration tone phases recorded during the precalibration period of the June 8, 1993, DOR measurement. Each point in this plot represents a group delay computed from a linear fit of five calibration tone phases to their baseband frequencies. Abrupt changes in the group delays of 10 to 15 nsec are seen in most of the DOR measurements and are likely caused by changes to the radio-frequency signal path that occur during the precalibration period as the receiving equipment is being prepared for the Mars Observer tracking pass.

Table 2 contains the estimated group delays computed from linear fits of the calibration tone phases to their baseband frequencies in each ETT channel. Each number represents the mean value taken over the indicated measurement interval. It is evident from these results that the group delays are quite sensitive to the number of calibration tones. In the first half of the MO DOR demonstration, only three tones were recorded in channel 2 of the ETT compared to five tones in channel 1. The delays computed using only three tones (before July 4, 1993) differ in magnitude from the delays computed with five tones by as much as 30 to 50 nsec. After July 4, 1993, when five tones were recorded in both ETT channels, the group delays in each channel are much more consistent with an average difference of approximately 3.2 nsec, on the same order as the variation in the channel group delays between DOR measurements. These problems are not completely understood, but are probably related to the errors in the calibration tone phases measured by the ETT mentioned above. Because of this, it was decided not to use the group delays computed from the phase-calibration tones to calibrate the instrumental delay term, $\Delta\tau_I$ of Eq. (3), but rather to assume that it would contribute a constant bias along with the other uncalibrated delay terms in this equation.

⁶ Ibid.

C. ETT Channel Phase Offset

A noninteger phase offset was found to exist between the two baseband channels of the experimental tone tracker at Canberra. This is apparent when spacecraft group delays are computed from the measured phases of the spacecraft tones and is manifest as a systematic difference in the magnitude of the group delays computed from tones within a single channel compared with those computed using tones in different ETT channels. The magnitude of the ETT channel phase offset at Canberra can be estimated from the phase-calibration data recorded immediately before each DOR pass by examination of residuals to linear fits of calibration tone phase to frequency.

Figure 12 shows residuals from a linear fit of calibration tone phase and frequency for data taken on August 15, 1993, at Goldstone and Canberra. These data indicate a phase offset of 0.27 cycle for the ETT at Canberra. There does not appear to be a significant phase offset between the channels of the ETT at Goldstone.

VI. Comparison With Conventional Δ DOR Measurements

Figure 13 shows the uncalibrated delay residuals for all successful DOR measurements that were completed during the first 8 months of 1993 (Table 1). No Rogue GPS clock solutions were available on June 8, 1993. The GPS clock solutions on days June 15, 1993 (day number 166), June 19, 1993 (day number 170), and June 23, 1993 (day number 174), are believed to be corrupted by bad timing offset measurements (see Section IV). As expected, these residuals show a significant signature due to the presence of instrumental and clock delays. That the majority of this signature is due to the clock offset between the DSN antennas is evident by comparing the general trend of the DOR delay residuals with the clock offsets estimated from GPS data that are also shown in this figure. Figure 14 shows the corrected DOR delay residuals produced by subtracting the clock offsets obtained from the GPS data that include the timing offset, τ_R , that relates the GPS clock to the station master clock. All delays in this figure correspond to the most widely separated tone pair ($\Delta\nu = 23.1$ MHz). The large biases in the quasar-free group delays are due to uncalibrated instrumental effects. The parentheses around the DOR points in this figure indicate that the GPS clock offsets for these points were computed by interpolation from nearby clock offsets. This was necessary because of problems in the timing offset measurements on these days (Section IV).

According to Eq. (3), the DOR delay residuals shown in Fig. 14 can be represented by

$$\begin{aligned} \delta\tau_{DOR}(\nu_i, \nu_j; t) &= \tau_{DOR}(\nu_i, \nu_j; t) - \tau_{DOR}^0 - \Delta\tau_C(t) \\ &= \Delta\tau_{FE}(\nu_i, \nu_j; t) + \Delta\tau_I(\nu_i, \nu_j; t) \\ &\quad - \Delta\tau_E(t) + \Delta\tau_{misc}(t) + \eta(t) \end{aligned} \quad (7)$$

where the δ designates a residual delay. In so far as the quantities on the right side of Eq. (7) are constant, the residual DOR delay, $\delta\tau_{DOR}$, should remain constant, and, in so far as these quantities are antenna pair dependent, so should the residual DOR delays be antenna dependent. That this is so is obvious from Fig. 14, where the residual DOR delays clearly fall into groups corresponding to the antenna pair used in the measurement.

The variations in the magnitudes of the residual delays, expressed as a sample standard deviation about the mean for the three antenna pairs used in this demonstration, are shown in Fig. 14 along with the unbiased Δ DOR delays. The scatter in the DOR delay residuals is about 5 to 7 nsec, albeit for rather small sample sets. The “flatness” of the DOR residuals is encouraging since it confirms our assumption that variations in the instrumental and miscellaneous delays and timing offsets remain relatively constant over long periods of time.

However, a delay measurement with a precision of 5 to 7 nsec, corresponding to an angular precision of approximately 250 to 350 nrad, would not provide a useful spacecraft navigation data type. The origin of this poor precision must lie in one of the terms on the right side of Eq. (7). For example, the formal errors on the Rogue receiver clock offsets, $\Delta\tau_{GPS}$, are less than 1 nsec, but the scatter in the timing offset measurement, τ_R , that relates the GPS clock to the station master clock, τ_C , is about 1.5 to 2.0 nsec. As mentioned earlier (Section V.A), there are also indications that strict configuration control was not applied to the τ_R calibrations by the DSN station personnel at Goldstone,⁷ but it is unclear what this might have contributed to the scatter in the timing offsets.

An assumed variation of 2.0 nsec in the $\Delta\tau_C$ term still leaves a delay scatter of 3 to 6.7 nsec. The most likely origin of this scatter lies in variations of the instrumental delay, $\Delta\tau_I$. Indeed, the group delays computed from the

⁷ M. Manning, op. cit.

phase calibration tones in Table 2 show variations on this order.

Variations in the phase offset between the ETT channels, discussed in Section V.C, could introduce additional noise into the delays computed from spacecraft tone pairs if each tone were in a different channel. However, a comparison of residual delays computed using the two side tones with 7.4-MHz separation in ETT channel 1 (Fig. 5) with those computed from the most widely spaced tone pair (23.1 MHz) where each tone lies in a different ETT channel shows that the delay variation due to the phase offset is only approximately 0.5 nsec, and cannot be responsible for the observed scatter in the residual delays of Fig. 14.

VII. Summary and Conclusions

The primary goal of the Mars Observer DOR demonstration was to assess the feasibility of measuring spacecraft angular position with 50-nrad accuracy without the need for an additional quasar observation. Spacecraft differential range measurements with approximately 0.2-nsec precision (i.e., DOR measurements) were obtained in near-real time using a new closed-loop receiver (experimental tone tracker) at each Deep Space Station. As expected (Section II.B), comparisons of the DOR measurements with simultaneous conventional Δ DOR measurements of the Mars Observer spacecraft show a large but constant bias due to uncalibrated instrumental delays and timing offsets. The DOR delays fall into groups corresponding to the particular antenna pair used in the DOR measurement. Within each group, the variation in the delay residuals over the course of the 5-month demonstration ranges from 3 to 7 nsec (Fig. 14).

This relatively large scatter in the DOR delay residuals is believed to result primarily from uncalibrated variations in the instrumental delays of the receiving systems at each complex. Although measurements of the phase-calibration tones should have been able to compensate for these variations, the station instrumental delays were not measured well in this demonstration (Section V.B). The calibration

tone-phase data that were obtained, however, are consistent with delay variations of this order (Table 2).

The station instrumental delay calibrations could be improved by

- (1) Improving the reliability of the station phase-calibration system (calibration data in this demonstration were obtained in less than 60 percent of the scheduled measurements).
- (2) Maintaining a constant tone power level during every measurement (configuration control).
- (3) Reducing the total number of tones in each channel by using a wider tone spacing in the phase-calibration tone generator [7].
- (4) Modifying the ETT to use 8-bit sampling of the signal.
- (5) Modifying the ETT to use an 8-bit phase model in the tone stopping function.

None of the above items presents serious technical challenges, and they are well within the capability of the DSN. The 8-bit data sampling and stopping function have already been implemented in similar hardware developed as part of the Galileo antenna arraying project.⁸ The overall station-pair-dependent DOR delay bias could be determined by occasional Δ DOR measurements since that part of the bias is expected to remain constant. Δ DOR measurements on one spacecraft should suffice to determine this bias for DOR measurements on other spacecraft.

Finally, it should be mentioned that one of the results of this work is the demonstration of interstation time synchronization at the subnanosecond level (Section IV). Although this was not the primary goal of the Mars Observer DOR demonstration, it is a necessary part of the DOR concept, and in itself constitutes an important result.

⁸ D. H. Rogstad, personal communication, Tracking Systems and Applications Section, Jet Propulsion Laboratory, Pasadena, California, February 18, 1994.

Acknowledgments

It would have been extremely difficult to complete the DOR measurements described here without the experimental tone tracker and the many individuals who contributed to the design, construction, and installation of this equipment at Goldstone and Canberra; these included Elliot Sigman of the Processor Systems Development Group and Jeff Srinivasan and Scott Stephens of the GPS Systems Group. Larry Young participated in helpful discussions during the preparation of this article. Individuals at the Deep Space Stations at Goldstone and Canberra provided the timing offset measurements, and Dave Jefferson of the Earth Orbiter Systems Group provided the Rogue GPS clock solutions from the FLINN analysis.

References

- [1] D. W. Curkendall and S. R. McReynolds, "A Simplified Approach for Determining the Information Content of Radio Tracking Data," *Journal of Spacecraft and Rockets*, vol. 6, no. 5, pp. 520–525, May 1969.
- [2] J. S. Border, F. F. Donovan, S. G. Finley, C. E. Hildebrand, B. Moultrie, and L. J. Skjerve, "Determining Spacecraft Angular Position With Delta VLBI: The Voyager Demonstration," Paper 82-1471, AIAA/AAS Astrodynamics Conference, San Diego, California, August 9–11, 1982.
- [3] J. S. Border and J. A. Koukos, "Technical Characteristics and Accuracy Capabilities of Delta Differential One-Way Ranging (Δ DOR) as a Spacecraft Navigation Tool," *Proceedings of the Meeting of the Consultative Committee for Space Data Systems on Radio Frequency and Modulation Standards Approval*, Munich, Germany, September 20, 1993 (in press).
- [4] K. M. Liewer, "DSN Very Long Baseline Interferometry System Mark IV-88," *The Telecommunications and Data Acquisition Progress Report 42-93*, vol. January–March 1988, Jet Propulsion Laboratory, Pasadena, California, pp. 239–246, May 15, 1988.
- [5] C. E. Dunn, S. M. Lichten, D. C. Jefferson, and J. S. Border, "Subnanosecond GPS-Based Clock Synchronization and Precision Deep Space Tracking," *The Telecommunications and Data Acquisition Progress Report 42-111*, July–September 1992, Jet Propulsion Laboratory, Pasadena, California, pp. 1–9, November 15, 1992.
- [6] J. F. Zumberge, D. C. Jefferson, G. Blewitt, M. B. Heflin, and F. H. Webb, "Jet Propulsion Laboratory IGS Analysis Center Report, 1992," *Proceedings of the 1993 IGS Workshop*, G. Beutler and E. Brockmann, eds., Astronomical Institute, University of Berne, pp. 154–163, 1993.
- [7] J. B. Thomas, "The Tone Generator and Phase Calibration in VLBI Measurements," *The Deep Space Network Progress Report 42-44*, vol. January and February 1978, Jet Propulsion Laboratory, Pasadena, California, pp. 63–74, April 15, 1978.

Table 1. Summary of Mars Observer DOR measurements.^a

Experiment times			Antenna		Phase calibration		GPS clock offset (DSCC 10/DSCC 40), nsec	Residual delay ($\Delta\nu = 23.1$ MHz), nsec ^b
DOY	Start	Stop	DSCC 10	DSCC 40	DSCC 10	DSCC 40		
80	0540	0620	14	45	No	Yes	2198.773	537.9569
93	0500	0540	15	45	Yes	No	2221.496	413.5409
147	0530	0610	14	45	Yes	Yes	1775.489	115.675
150	0510	0550	14	45	Yes	Yes	1772.710	118.385
159	0435	0515	14	45	Yes	Yes	— ^c	121.562
166	0420	0500	15	43	No	Yes	2832.140	90.711
170	0405	0445	14	45	Yes	Yes	2247.283	100.95
174	0200	0240	14	45	Yes	No	2241.790	98.74
178	0425	0505	15	43	No	Yes	1756.806	58.725
185	0215	0255	14	45	No	Yes	1729.440	65.64
199	0320	0400	15	43	Yes	No	1728.658	21.906
206	0255	0335	15	43	Yes	Yes	1694.939	4.499
213	0100	0140	15	43	Yes	Yes	1684.606	-8.735
219	0035	0115	15	43	Yes	Yes	1662.329	-34.839
227	0235	0315	15	45	Yes	Yes	1626.346	67.742
228	0230	0310	15	43	Yes	Yes	1623.552	-75.187

^a Includes only those measurements where spacecraft signal was acquired at both stations.

^b Difference between observed and model delay.

^c No GPS clock offset available on this day.

Table 2. Summary of ETT instrumental group delays.

Phase calibration measurement interval			ETT channel group delay, nsec							
			DSS 14		DSS 15		DSS 43		DSS 45	
DOY	Start	Stop	Ch 1	Ch 2	Ch 1	Ch 2	Ch 1	Ch 2	Ch 1	Ch 2
The following measurements used five phase-calibration tones in ETT channel 1 and three tones in ETT channel 2										
80	0446	0451							-5930.58	-5896.97
92	2318	2323			-5234.54	-5219.14				
147	0518	0519	-3296.37	-3356.80					-5930.59	-5932.58
147	0431	0436								
150	0451	0456	-3288.76	-3277.38					-5293.45	-5970.15
150	0338	0342								
159	0418	0423	-3296.54	-3361.55					-5929.61	-5968.96
159	0223	0228								
166	0358	0403					-3391.83	-3399.62		
170	0336	0341	-3291.58	-3273.43					-5927.88	-5976.65
170	0346	0349								
174	0127	0131	-3296.27	-3233.94						
178	0400	0403					-3393.01	-3402.87		
The following measurements used five phase-calibration tones in each ETT channel										
185	0146	0148							-5930.56	-5925.18
199	2101	2104			-5234.62	-5237.89				
206	1756	1759			-5222.15	-5232.48				
206	0234	0239					-3395.34	-3396.64		
213	1600	1605			-5235.38	-5236.14				
213	0128	0133					-3393.21	-3392.58		
219	1647	1652			-5234.23	-5234.25				
219	0026	0031					-3400.97	-3402.43		
227	1706	1708			-5222.97	-5234.52				
227	0204	0209							-5930.71	-5930.11
228	1901	1906			-5238.23	-5237.86				

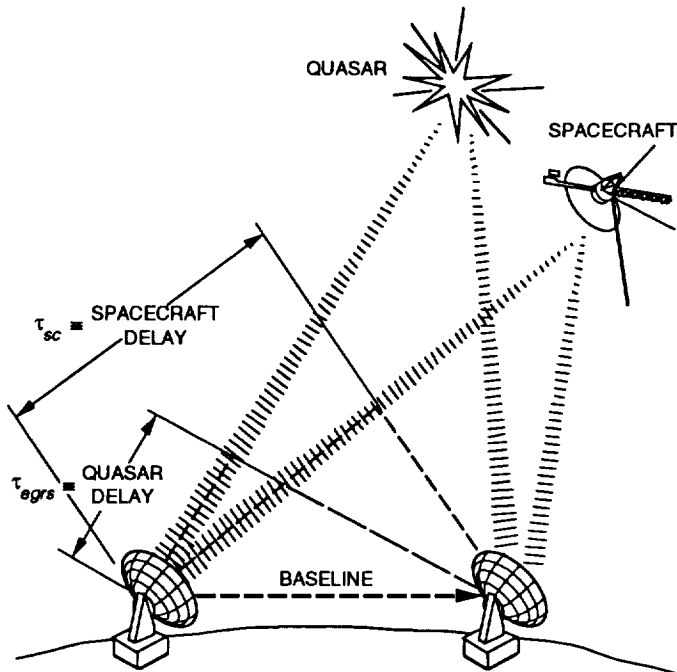


Fig. 1. Geometry of a typical Δ DOR observation.

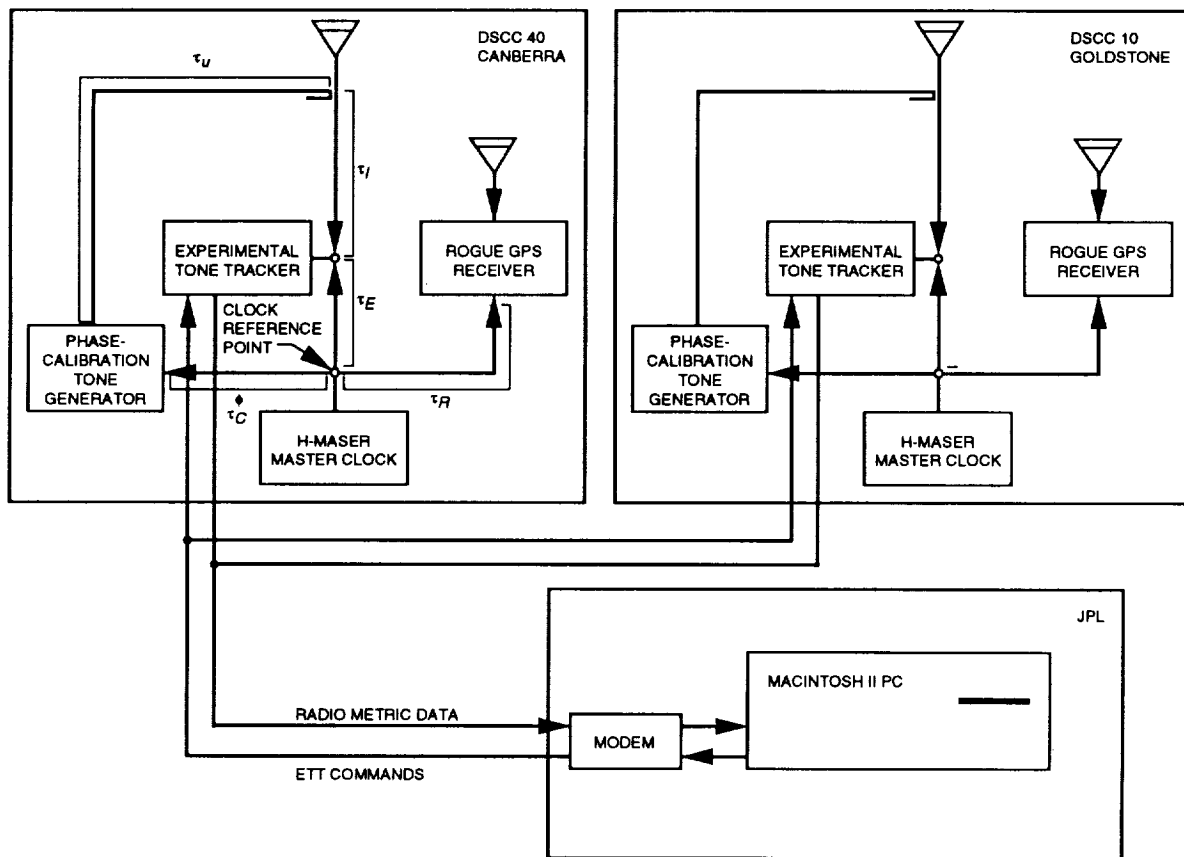


Fig. 2. Experimental setup used at DSCC 10 and DSCC 40 during the Mars Observer DOR demonstration. Various Instrumental timing offsets are defined in Section V.

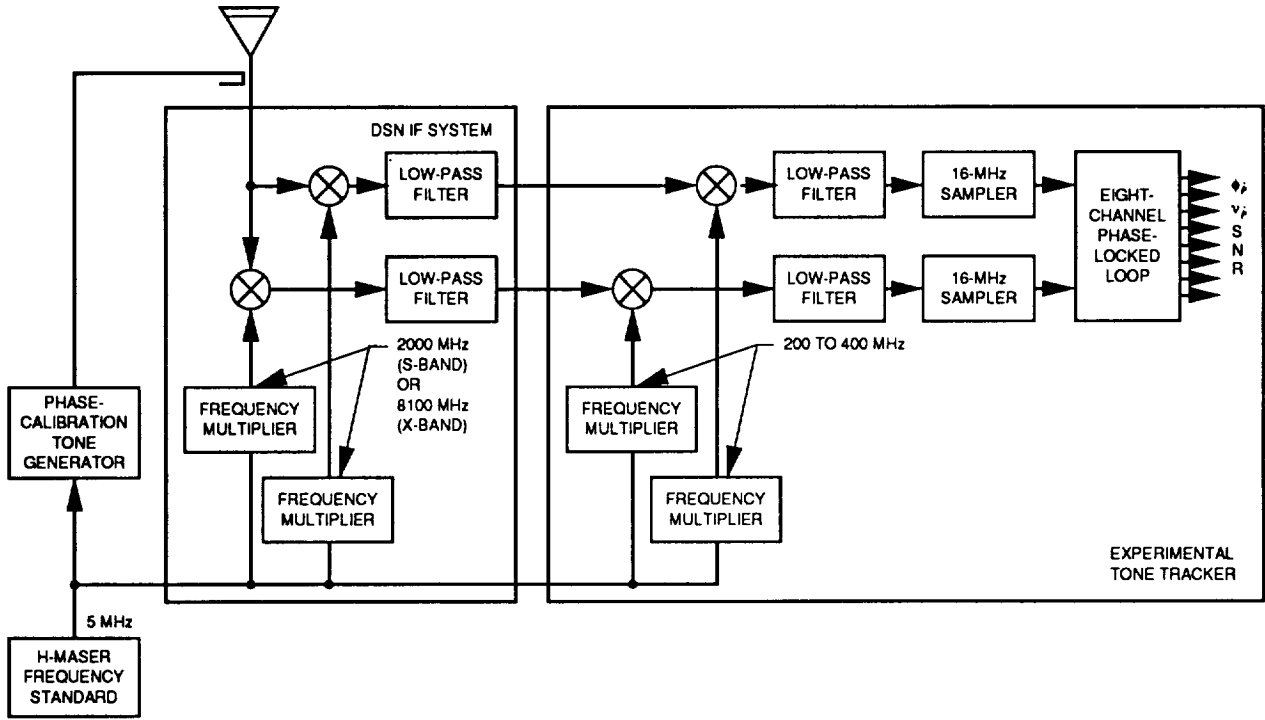


Fig. 3. The ETT tone tracker and its connection to the DSN antenna receiving system.

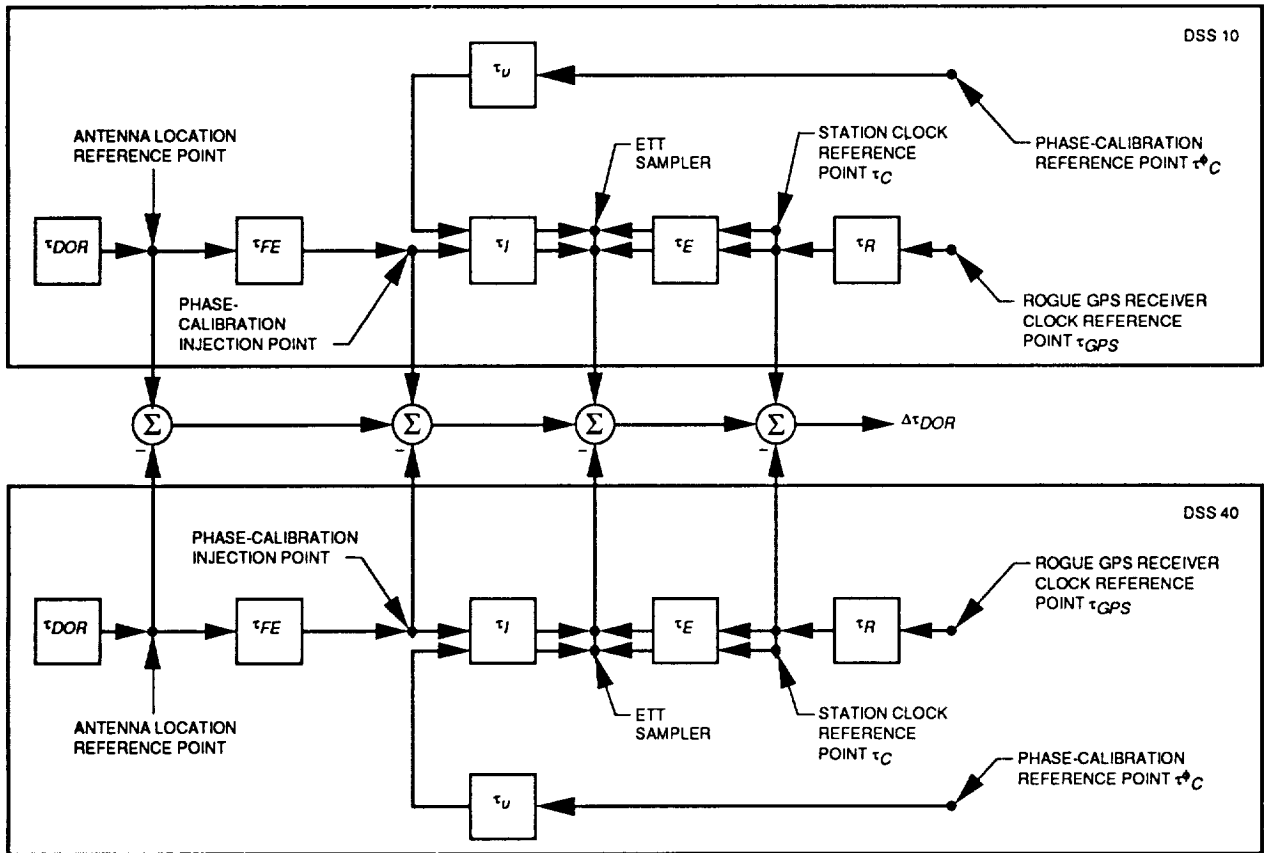


Fig. 4. Instrumental delay terms and timing offsets that contribute to the DOR delay observable of Eq. (3).

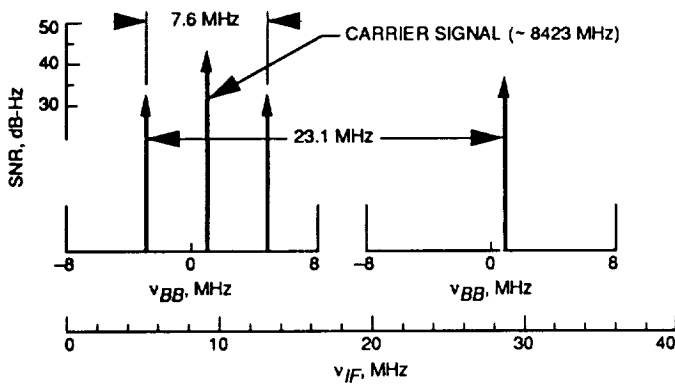


Fig. 5. Location of carrier signal and DOR tones recorded by the ETT during the Mars Observer DOR demonstration. The height of the arrows represents the relative signal-to-noise ratio of the tones.

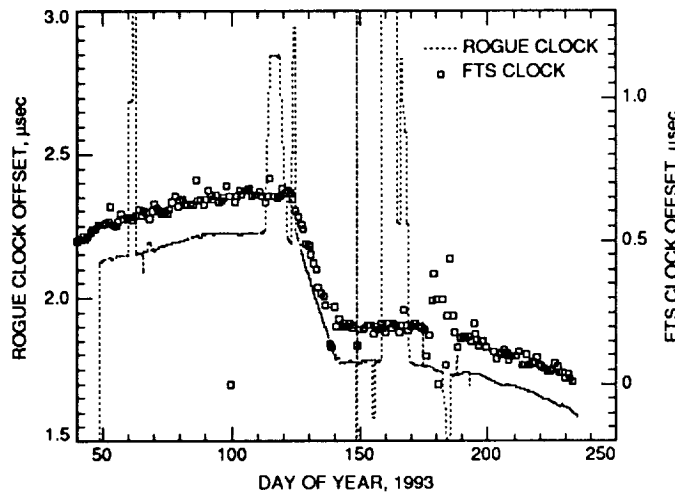


Fig. 6. Comparison of station clock offsets determined from the DSN's FTS system and those determined from the Rogue GPS receivers.

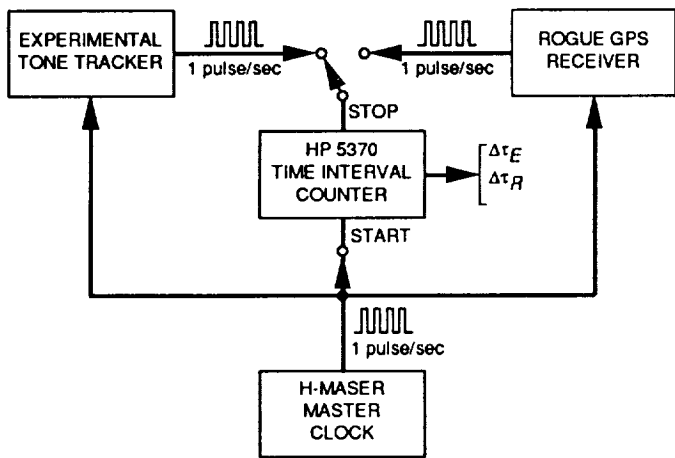


Fig. 7. Timing measurements performed at DSCC 10 and DSCC 40 to determine the time difference between the station master clock and the ETT and Rogue GPS receiver.

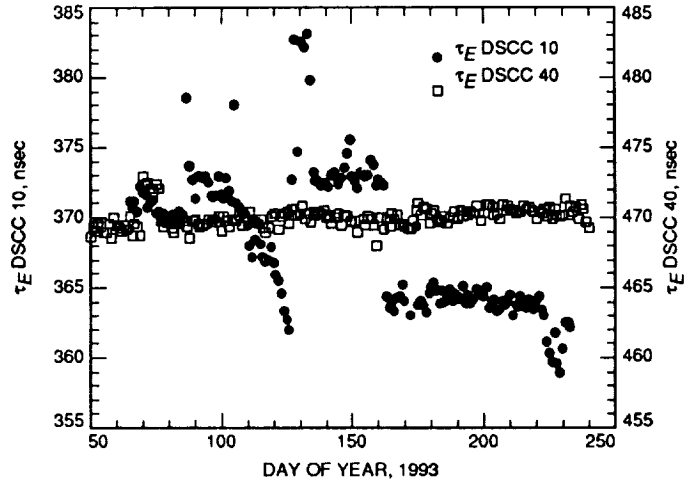


Fig. 8. Results of timing offset measurements for the τ_E delay of Eq. (3).

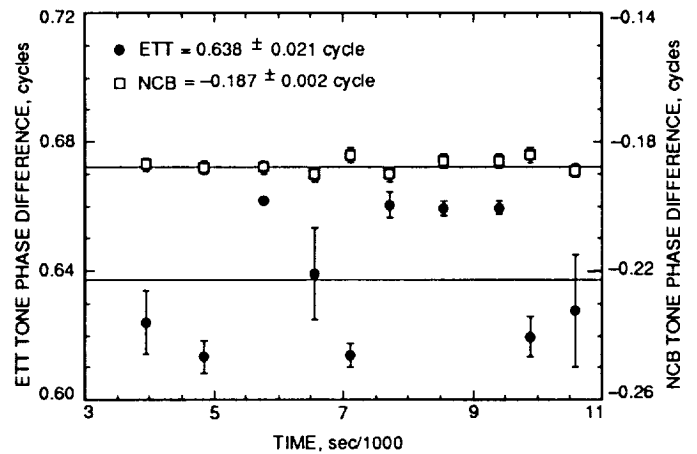


Fig. 9. Tone phase differences for the same pair of calibration tones recorded on May 19, 1993, at DSS 45 by the ETT and the DSN narrow-channel bandwidth VLBI system.

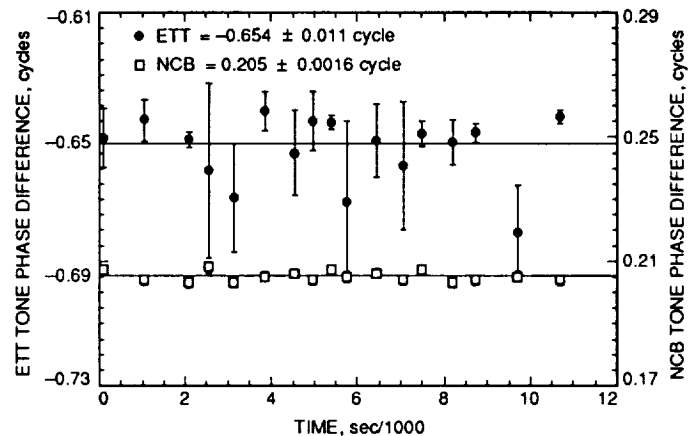


Fig. 10. Tone phase differences for the same pair of calibration tones recorded on March 24, 1993, at DSS 15 by the ETT and the DSN narrow-channel bandwidth VLBI system.

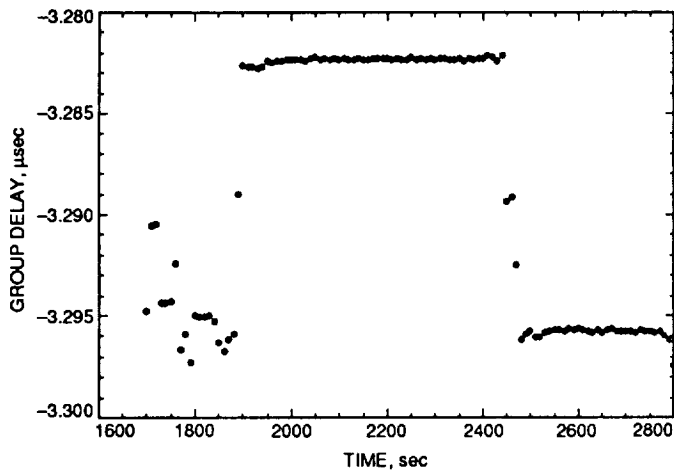


Fig. 11. Instrumental group delays computed from linear fits of tone phase versus frequency plots.

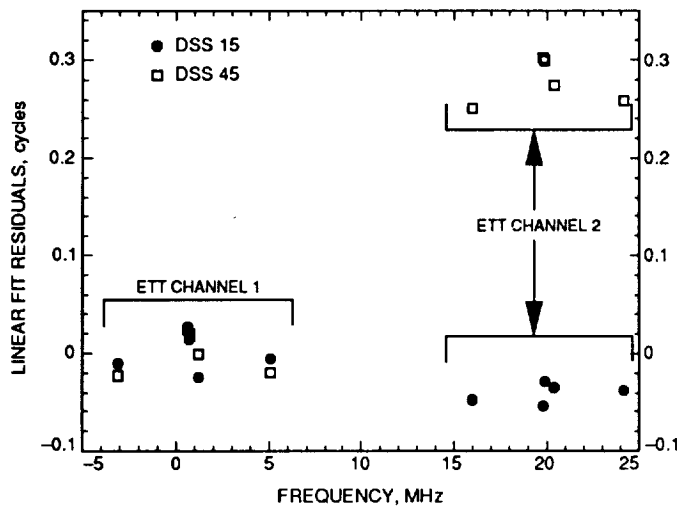


Fig. 12. Typical residuals to linear fit of phase calibration tone phases to frequency for both channels of the ETT.

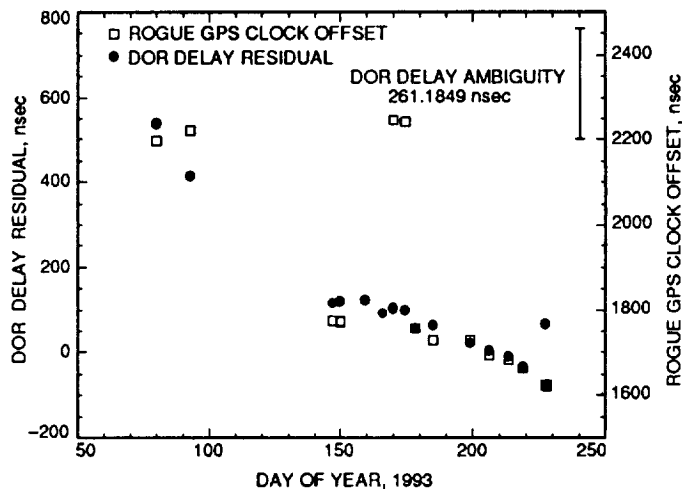


Fig. 13. Comparison of quasar-free DOR group delay residuals corresponding to the most widely separated spacecraft tone pair and station timing offsets estimated from the Rogue receiver GPS data.

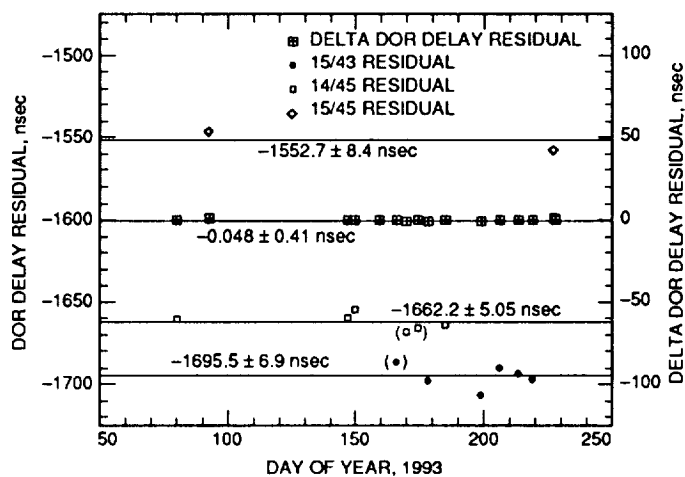


Fig. 14. Comparison of group delay residuals from the conventional Δ DOR measurements of Mars Observer and the group delay residuals from the quasar-free DOR measurements.

32
1-13

Influence of an Externally Modulated Photonic Link on a Microwave Communications System

X. S. Yao and L. Maleki
Communications Systems Research Section

We analyze the influence of an externally modulated photonic link on the performance of a microwave communications system. From the analysis, we deduce limitations on the photocurrent, magnitude of the relaxation oscillation noise of the laser, third-order intercept point of the preamplifier, and other parameters in order for the photonic link to function according to the system specifications. Based on this, we outline a procedure for designing a photonic link that can be integrated in a system with minimal performance degradation.

I. Introduction

Photonic technology has become increasingly important in analog communications systems. For systems with high frequency and high dynamic range, externally modulated photonic links generally have better performance compared to directly modulated links [1,2]. The performance of such links has been analyzed by many authors [3-6]; however, in these analyses the links were assumed to be isolated from the microwave system and, therefore, their effect on the system was not adequately apparent. In addition, many parameters in these analyses were given for component engineers and, thus, are difficult to use for a system designer, who may not be familiar with the photonic technology. Finally, none of the analyses considered the influence of the laser's relaxation oscillation noise amplitude on the microwave system, which, as will be discussed later, may be critical in many applications.

We present here an analysis that emphasizes the integration of the link in an analog system. We pay spe-

cial attention to the laser's relaxation oscillation noise and determine quantitatively its effect on the system. With parameters and equations intentionally written in system engineering terms, we hope that the results can be readily used by microwave engineers in their system designs.

An analog communications system can be considered as many subsystems that are cascaded together. Each subsystem i has a characteristic gain G_i , noise factor F_i , 1-dB compression $P_i^{1\text{dB}}$, third-order intercept point IP_i , and bandwidth Δf_i . Grouping the subsystems is somewhat arbitrary; for convenience, we group the system under consideration into three subsystems, as shown in Fig. 1. All the components before the optical link are included in subsystem 1, and all the components after the optical link are included in subsystem 3. The optical link itself is subsystem 2. For example, in an antenna remote system where the optical link is inserted between the low-noise amplifier (LNA) of the antenna and the downconverter, subsystem 1 is the LNA and subsystem 3 includes the downconverter